New Journal of Chemistry

On the reactivity of manganese dioxide with different substrates in organic solvents

Angelo Alberti, Paola Astolfi,* Patricia Carloni, Lucedio Greci, Corrado Rizzoli, Pierluigi Stipa

Content of Supporting Information.

ESR characterization of nitroxides 4-6.

Discussion on radical cation 8 formation.

Crystal structure of 3'b.Details of the X-ray data collection and structure analysis. Brief description of the structure. Content of the asymmetric unit and packing diagram (2 figures). Table S2: experimental data for the X-ray diffraction studies, Table S3: selected bond lengths and angles; Table S4: hydrogen bonding interactions.

ESR characterization of nitroxides 4-6.

Quinonimine *N*-Oxides **2'a**, **2'b**, **2"a**, **2"b**, **3'a**, and **3'b** isolated in the reaction between nitroxides **2-3** and MnO_2, when crystallised from hot ethanol contain traces of the correponding hydroxy-substituted nitroxides **4a**, **4b**, **5a**, **6a** and **6b** as shown in Scheme S1 as already repoerted in the literature.[1] Hyperfine coupling constants and *g*-factors for nitroxides **4-6** are collected in Table S1

Table S1 EPR spectral parameters for nitroxide radicals **4-6**

Compound	**Nitroxide**	**Hfs**[a] / mT	***g***
2'a	**4a**	0.987(1N), 0.303(1H), 0.095(2H), 0.087(1N)	2.0052_6
2'b	**4b**	0.966(1N), 0.3081(H), 0.107(2H), 0.084(1N)	2.0055_3
2"a	**5a**	1.072(1N), 0.330(1H), 0.095(2H) 0,086(1N)	2.0054_2
2"b	**5b**	1.050(1N), 0.340(1H), 0.096(2H), 0.084(1N), 0.047(1H), 0.051(1H)	2.0050_9
3'a	**6a**	1.045(1N), 0.312(1H), 0.099(3H)	2.0055_3
3'b	**6b**	1.022(1N), 0.308(1H), 0.115(1H), 0.094(1H), 0.081(1H)	2.0046_9

[a] Hfs: Hyperfine splittings

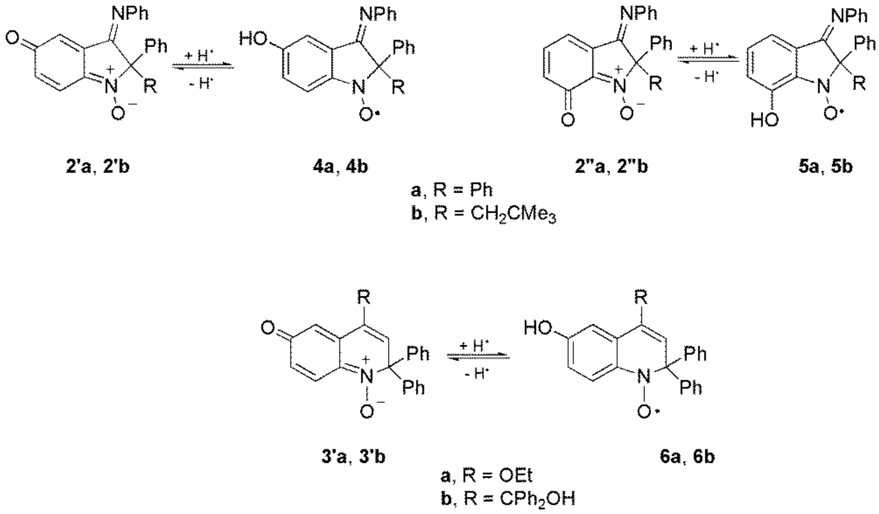

Scheme S1. Origin of adventitious nitroxides **4-6**

Discussion on radical cation 8 formation.

When *p*-anisidine **7** and MnO_2 were reacted inside the EPR, a signal was recorded only after addition of traces of *p*-toluensulphonic acid. This signal was characterized by a six line pattern superimposed to a strong single line which could be due either to radical cation $ArNH_2^{+\bullet}$ or to the aminyl radical $ArNH^{\bullet}$.

Radical cations of substituted anilines are characterized by complex spectra, with overall splitting normally larger than 5.0 mT and *g*-factor values in the range 2.0025 to 2.0035,[2,3] while aminyl radicals from substituted anilines show in turn overall splittings larger than 3.5 mT and *g*-factor values in the range 2.0030 to 2.0037.[4,5] An additional puzzling point that we cannot fail to note, is that a virtually identical spectrum has been previously observed when reacting manganese dioxide with methyl (2*E*)-2,3-bis(3,4-dimethoxyphenyl)acrylate in trifluoroacetic acid.[6] While the reasonable doubt might then rise that the EPR observation depends exclusively on MnO_2 and the acidic medium, without involving the organic counterpart (in our case *p*-anisidine), we found that the addition of *p*-toluensulphonic acid in MeCN to an oxygen-free benzene suspension of MnO_2 did not lead to the observation of any EPR signal.

All in all, we believe that the spectrum shown in Figure 3 (see text) can be rationalized when bearing in mind that the occurrence of electron spin exchange between radicals causes a broadening of the spectral lines that, if the exchange is very substantial, may eventually collapse to a single line, as it is the case for most pure solid free radicals.[7] Hence, we assign the six line spectrum to a Mn(II) species and the single line to the radical cation **8** formed on the surface of MnO_2 grains suspended in the medium, the two paramagnetic species being formed as indicated in reaction S1.

$$MnO_2 + ArNH_2 \rightarrow MnO^{-\bullet} + ArNH_2^{+\bullet} + \tfrac{1}{2}\, O_2 \qquad \text{(S1)}$$

As for the Mn(II) species, this might be the radical anion of MnO (see reaction S1) or, more likely, the Mn(II) salt of *p*-toluensoulphonic acid. To check whether the latter was indeed the case it was decided to examine an authentic sample of Manganese(II) *p*-toluenesulphonate. Since this compound is not commercial, we dissolved some Mn(II) acetate in acetonitrile/benzene (some water was also needed to achieve dissolution, see Experimental) and then added an excess of *p*-toluensulphonic acid. When inserted in the spectrometer cavity the solution exhibited a strong EPR spectrum characterized by $a_{Mn(II)}$ = 9.41 mT and $g = 2.0099_5$, fairly similar to those observed for the six line signal afforded by the MnO_2/*p*-anisidine system. Although, there is little doubt that, due to the relative strength of acetic and *p*-toluensulphonic acids, a displacement reaction would occur leading to the in situ formation of Mn(II) *p*-toluenesulphonate, exactly the same spectrum was exhibited by a similar solution of Mn(II) acetate alone, which seems to indicate a negligible effect of the counterion on the EPR spectral parameters. To some extent, this was an unexpected finding, but we nevertheless believe that these EPR experiments provide support to our proposed mechanism.

Crystal structure determination of quinoneimine *N*-oxide 3'b (Fig. S1)

Single crystals of **3'b** were recrystallised from ethanol, mounted on a glass fibre and transferred to a Siemens AED diffractometer. Crystal data. $C_{34}H_{25}NO_3$, M = 947.66, monoclinic, a = 12.8819(11), b = 19.3135(15), c = 21.382(3) Å, β = 94.830(9), U = 5300.8(10) Å^3, T = 295 K, space group $P2_1/c$ (no.14), Z = 8, 21033 reflections measured, 10048 unique (R_{int} = 0.028) which were used in all calculations. The final $wR(F_2)$ was 0.127 (all data) and R was 0.045 (for 6343 reflections having $I > 2\sigma(I)$).

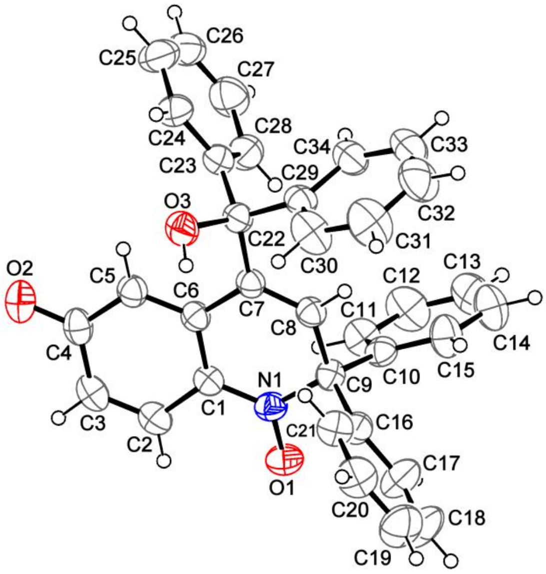

Fig. S1 - The molecular structure of one independent molecule of compound **3'b**. Displacement ellipsoids are drawn at the 40% probability level.

Details of the X-ray data collection, structure solution, and refinement for compound 3'b.

A pale yellow, prismatic crystal suitable for X-ray analysis was mounted on a glass fibre. Data were collected on a three-circle Siemens AED diffractometer using graphite-monochromatized Cu-$K\alpha$ radiation at 295(2) K. Data reduction was carried out by the AED[8] program. No correction for absorption was applied.

The function minimized during the least-square refinement was $\Sigma w(\Delta F^2)$.[9] Anomalous scattering corrections were included in structure factor calculations. Structure solution was based on the observed reflections $[I>2\sigma(I)]$ while the refinements were based on all unique reflections. The structure were solved by direct methods using SIR97.[9] Refinement was done anisotropically by full matrix least-squares for all non-H atoms using SHELXL-97.[10] The hydroxy H atoms were located in a different Fourier map and constrained to ride on their parent atoms using a rotating model (AFIX 87) with O–H = 0.82 Å and free isotropic displacement parameters. All other H atoms were positioned geometrically and constrained to ride with C–H = 0.93 Å and with $U_{\mathrm{iso}}(\mathrm{H}) = 1.2U_{\mathrm{eq}}(\mathrm{C})$. An outlier (-1 0 2) having $|I_o - I_c|/(I_o) < -100$ was omitted in the last cycles of refinement. Crystal data and details associated with data collection are given in Table S1.

Description of the structure

The asymmetric unit of compound **3'b** (Fig. S2) consists of two crystallographically independent molecules (C1-C34/O1-O3/N1 and C35-C68/O4-O6/N2, hereafter referred as molecules *A* and *B*) of similar geometry, the main difference consisting in orientation of the phenyl rings with respect to the quinoneimine *N*-oxide ring system.

The fused-ring system of both molecules is approximately planar (r.m.s. deviations 0.057 and 0.047 for *A* and *B*, respectively) and forms with the attached phenyl rings dihedral angles of 76.35(5) and 82.29(6)° in molecule *A*, and 62.17(6) and 77.96(6)° in molecule *B*. The dihedral angles between the aromatic rings of the diphenylmethanol fragments and the fused-ring systems are 84.97(5) and 81.80(6)° in molecule *A*, and 82.51(5) and 87.42(7)° in molecule *B*.

All bond lengths and angles (Table S2) are not unexceptional and deserve no further comment.

In the crystal structure (Fig. S2), molecules *A* and *B* are linked into a dimeric unit by a pair of intermolecular O–H...O hydrogen bonds (Table S4). The structure is further stabilized by intra- and intermolecular non-classical C–H...O hydrogen bonds (Table S4).

References

1 A. Alberti, R. Andruzzi; L. Greci; P. Stipa; G. Marrosu; A. Trazza and M. Poloni, *Tetrahedron*, 1988, **44**, 1503 and references reported therein.

2 S.F. Nelsen, in *Landolt-Börnstein: Magnetic Properties of Free radicals*, Fischer, H.; Hellwege, K.-H. Eds, *II/9d2*, pp. 22-123: Springer-Verlag, Heidelberg, 1979.

3 S.F. Nelsen, in *Landolt-Börnstein: Magnetic Properties of Free radicals*, Fischer, H. Ed., *II/17h*, pp. 122-245: Springer-Verlag, Heidelberg, 1990.

4 F.A Neugebauer, in *Landolt-Börnstein: Magnetic Properties of Free radicals*, Fischer, H.; Hellwege, K.-H. Eds, *II/9c1*, pp. 5-191: Springer-Verlag, Heidelberg, 1979.

5 F.A. Neugebauer, in *Landolt-Börnstein: Magnetic Properties of Free radicals*, Fischer, H. Ed, *II/17c*, pp. 387-642: Springer-Verlag, Heidelberg, 1987.

6 K. Wang; Y. Hu; Z. Li; M. Wu; Z. Liu; B. Su; A. Yu; Y. Liu; and Q.-M. Wang**,** *Synthesis*, 2010, **7**, 1083.

7 J.E. Wertz and J.R. Bolton in *Electron Spin Resoance. Elementary theory and application*, pp 201-203: McGraw-Hill Book Company, New York, 1972

8 D. Belletti; A. Cantoni and G. Pasquinelli, *AED Internal Report 1/93.*Centro di Studio per la Strutturisctica Diffrattometrica del CNR, Parma Italy; 1993

9 A. Altomare; M.C. Burla; M. Camalli; G. Cascarano; A. Guagliardi; A.G.G. Moliterni; G. Polidori and R. Spagna, *J. Appl. Cryst.*, 1999, **32**, 115.

10 G.M. Sheldrick, *Acta Cryst*., 2008, **A64**, 112.

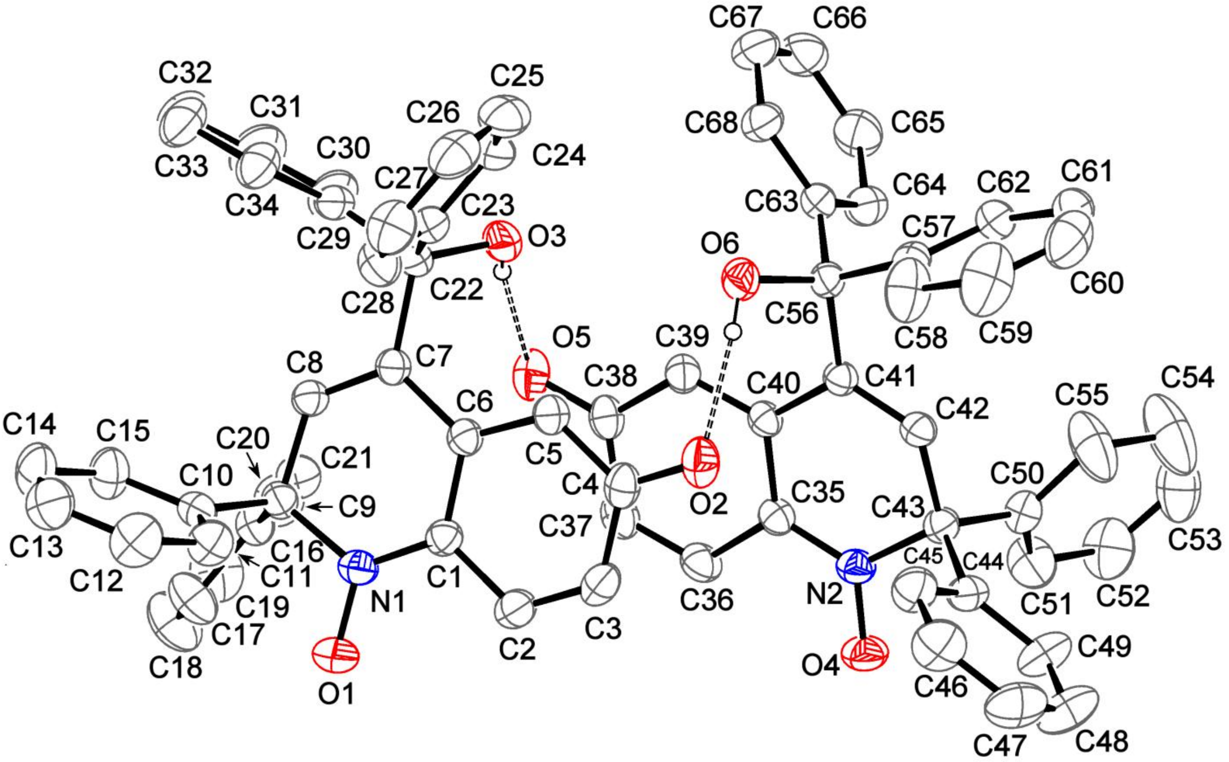

Fig. S2. The asymmetric unit of **3'b** with displacement ellipsoids drawn at the 50% probability level. O–H...O hydrogen bonds are shown as dashed lines.

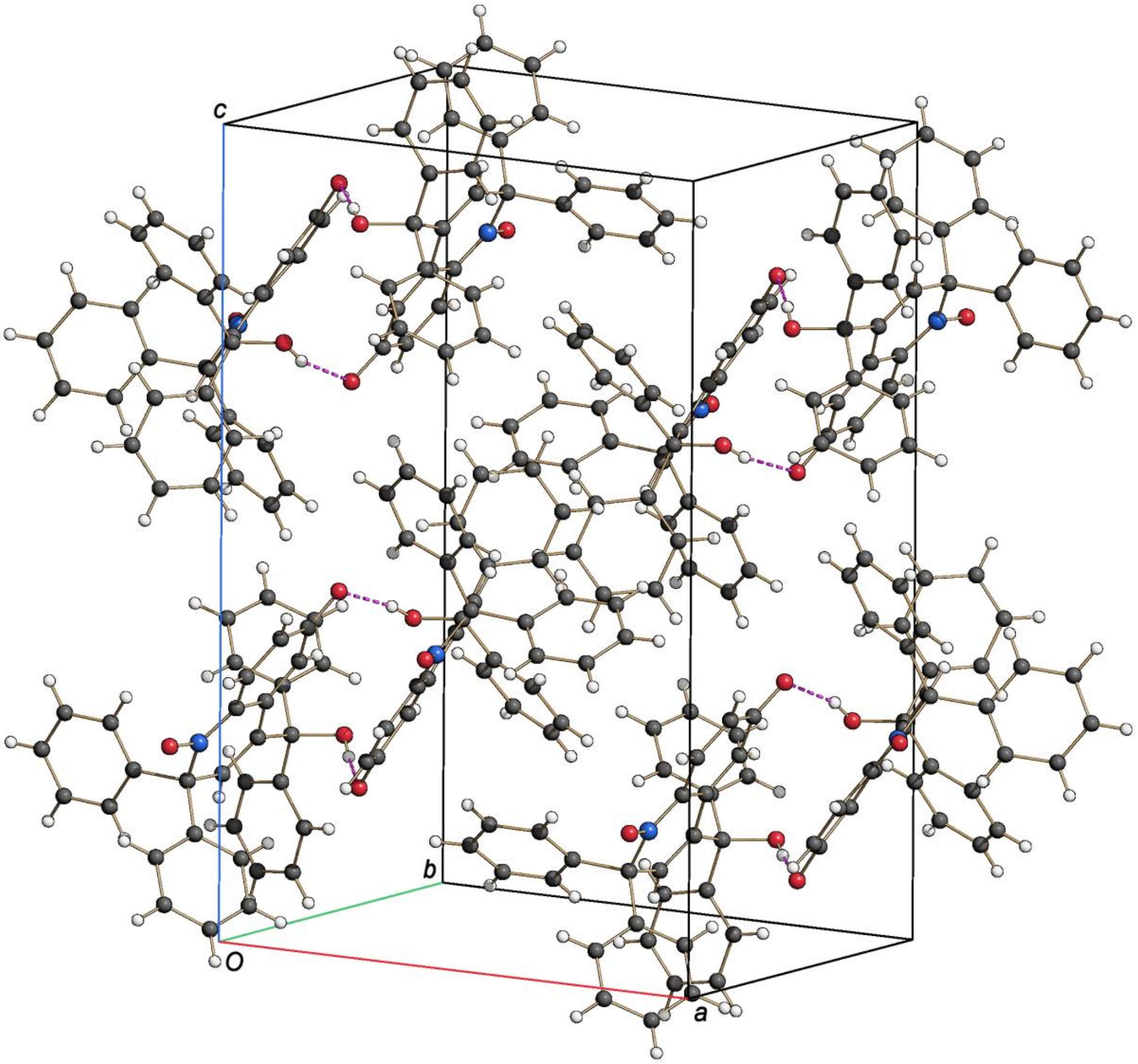

Fig. S3 Packing diagram of **3'b**. Intermolecular O–H...O hydrogen bonds are shown as dashed lines.

Table S2. Experimental Data for the X-ray Diffraction Studies on Crystalline Compound **3'b**.

Formula	$C_{34}H_{25}NO_3$
Formula weight	495.55
Crystal habit	block
Crystal colour	pale yellow
Crystal dimension, mm	0.17 x 0.20 x 0.27
Crystal system	monoclinic
Space group	$P2_1/c$
Cell parameters:	
a, Å	12.8819(11)
b, Å	19.3135(15)
c, Å	21.382(3)
β, °	94.830(9)
V, Å^3	5300.8(10)
Z	8
D_{calc}, Mg m^{-3}	1.242
Linear absorption coefficient, mm^{-1}	0.628
Diffractometer	Siemens AED
Temperature, K	295
Radiation, Å	1.54178
Data collection range of 2θ, deg	6.18 - 140.02
Reflections measured	±h, k, ±l
Total data collected	20678
Unique total data	10048
Unique observed data	6343
Criterion for observation	$I > 2\sigma(I)$
Unique data used in the refin. (NO)	10048
Number of parameters refined (NV)	689
Overdetermination ratio (NO/NV)	14.6

Table S2. Experimental Data for the X-ray Diffraction Studies on Crystalline Compound **3'b** (cont.).

$R = \Sigma\vert\Delta F\vert / \Sigma\vert F_o\vert$ [a]	0.045
$wR2 = [\Sigma w\vert\Delta F^2\vert^2 / \Sigma w\vert Fo^2\vert^2]^{1/2}$ [b]	0.127
$GOF=[\Sigma w\vert\Delta F^{2\vert 2} / (NO\text{-}NV)]^{1/2}$	0.958
Largest shift/esd, final cycle	<0.001
Largest peak/hole, e/$Å^3$	0.14/-0.19

[a] calculated on the unique observed data.

[b] calculated on the unique data used in the refinement.

.

Table S3. Selected bond lengths (Å) and angles (°) for **3'b**.

O1–N1	1.2695(18)	O4–N2	1.2733(18)
O2–C4	1.248(2)	O5–C38	1.240(2)
O3–C22	1.430(2)	O6–C56	1.426(2)
N1–C1	1.336(2)	N2–C35	1.337(2)
N1–C9	1.504(2)	N2–C43	1.505(2)
C1–C2	1.437(2)	C35–C36	1.437(2)
C1–C6	1.448(2)	C35–C40	1.453(2)
C2–C3	1.336(3)	C36–C37	1.337(3)
C3–C4	1.447(3)	C37–C38	1.456(3)
C4–C5	1.449(2)	C38–C39	1.443(2)
C5–C6	1.357(2)	C39–C40	1.355(2)
C6–C7	1.470(2)	C40–C41	1.466(2)
C7–C8	1.327(2)	C41–C42	1.325(2)
C7–C22	1.547(2)	C41–C56	1.546(2)
C8–C9	1.496(2)	C42–C43	1.498(2)

O1–N1–C1	122.67(15)	O4–N2–C35	122.00(14)
O1–N1–C9	114.53(14)	O4–N2–C43	114.88(14)
C1–N1–C9	122.80(14)	C35–N2–C43	123.12(14)

Table S4. Hydrogen bonding interactions (Å, °) for **3'b**.

	D–H (Å)	H...A (Å)	D...A (Å)	D–H...A (°)
O3–H3O...O5	0.82	2.01	2.798(2)	160
O6–H6O...O2	0.82	1.96	2.771(2)	169
C5–H5...O3	0.93	2.49	2.981(2)	113
C33–H33...O4^{i}	0.93	2.48	3.317(3)	151
C39–H39...O6	0.93	2.50	2.995(2)	114
C45–H45...O2	0.93	2.59	3.513(3)	170
C48–H48...O4^{ii}	0.93	2.60	3.504(3)	164
C51–H51...O4	0.93	2.26	2.895(3)	125

Symmetry codes: (i) -x, 0.5+y, 0.5-z: (ii) 1-x, -y, 1-z